



Contents lists available at <http://qu.edu.iq>

Al-Qadisiyah Journal for Engineering Sciences

Journal homepage: <http://qu.edu.iq/journaleng/index.php/IQES>



Experimental study of natural convection heat transfer enhancement in a square cavity filled with nanofluid using magnetic effects

Noor S. Najem*, Hadi O. Basher, and Mohammed D. Salman

Mechanical Engineering Department, Wasit University, College Of Engineering, Iraq

ARTICLE INFO

Article history:

Received 15 May 2022

Received in revised form 14 June 2022

Accepted 22 July 2022

Keywords:

Natural Convection,
Heat Transfer,
Square Cavity,
Nanofluid,
Magnetic Effects.

ABSTRACT

Researchers in heat transfer are paying close attention to nanofluids because of their potential as high-performance thermal transport media. In light of natural convection's enormous significance, the addition of nanoparticles significantly enhances the thermophysical properties of the nanofluids compared to the base fluid. In this study, experimental work was used to evaluate the influence of CuO nanoparticles on natural convection with magnetohydrodynamic (MHD) flow in a square cavity. The cavity's left and right vertical walls were maintained at different temperatures, and the top and bottom walls of the cavity were insulated. This experimental study applied a horizontal magnetic field with uniform strength. Results were obtained for a variety of Hartmann numbers ranging from 0–300, Rayleigh numbers going from $2.76E+8$ to $6.89E+8$, and solid volume fractions ranging from 0 to 1.5% Vol. Results showed that the heat transfer coefficient and Nusselt number values decreased with the increase in the values of the Hartmann number, except for the heat transfer coefficients at $Ha=100$ and 150 are larger than the heat transfer coefficients at $Ha=0$. The maximum heat transfer coefficient and Nusselt number enhancement were 40.8% and 28.5%, respectively, at a 1.5% volume concentration of CuO-water nanofluid, $Ra=6.7E+8$ and $Ha=100$ compared with pure fluid (water) at $Ha=0$.

© 2022 University of Al-Qadisiyah. All rights reserved.

1. Introduction

In recent decades, there has been a growing recognition that fluid movements and transport processes caused or influenced by buoyancy are of interest and relevance in many scientific and technological domains, particularly in engineering and science. This topic is currently being discussed in conferences and journals that cover a wide range of issues, including meteorology, geophysics, astrophysics, nuclear reactor systems, materials processing, solar energy systems, energy storage and conservation, fire control, the chemical, food, and metallurgical industries, as well as the more traditional fields of fluid and thermal sciences, among

others. In order to meet the ever-increasing power requirements, it is imperative that every method of enhancing the efficiency of power-generating cycles be explored. Therefore, it's worth thinking about the working fluid utilized while improving the power cycle. In addition, there should be further research into whether nanofluids can be used in any thermal transport system due to their potential as a novel heat transfer fluid and their relative simplicity of integration into an existing design.

In recent decades, researchers have looked at using 'micro' or 'Nanosized particles to improve heat dispersion [1]. Solids have superior thermal conductivity properties to liquids. As a result, current scientific technology uses nanometer-sized solid particles, often with a diameter of less than 50

* Corresponding author.

E-mail address: noors301@uowasit.edu.iq (Noor S Najem)



nm. Choi [2] is the first to use the word Nanofluid, which refers to a colloidal mixing of nanoparticles and a base fluid that has been described before. The majority of the studies have demonstrated that metallic particles transmit more heat energy than non-metallic particles when compared to one another. Pordanjani et al., 2019 [3] investigated the effect of a heat source and its location on natural convection in a C-shaped enclosure saturated with a nanofluid. Different Rayleigh numbers (10^3 – 10^6) and solid volume percentages of the nanofluid were considered (0–0.05). The results show that the highest Nusselt number is achieved with the heat source in the top horizontal cavity at $Ra = 10^3$. Therefore, it is recommended to use high Rayleigh numbers ($Ra = 10^6$) and vertical cavities. High Rayleigh numbers cause the highest increase when the heat source is in the vertical axis's upper part. Mohebbi et al. 2019 [4] used the lattice Boltzmann approach to measure the heat transfer from a nanofluid thermogravitational enclosure to a local heater (LBM). The influence of the Rayleigh number (10^3 – 10^6), cavity aspect ratio (0.2–0.6), nanofluid solid volume fraction (0–0.05), heater height and placement, as well as other liquid circulation and heat transfer factors, were studied in this work. The mean Nusselt number climbed as the Rayleigh number and nanoparticle concentration grew. The mean Nusselt number is highest when the heater is on the left border, consistent with earlier studies. Izadi et al., 2018 [5] studied the natural convection of Cu-water nanofluid within a wavy wall enclosure with a cylindrical heater. The results indicated that raising the solution's temperature reduces homogeneity. Moreover, the average Nusselt number of both porous phases increases with the Brownian parameter but decreases with the thermophoresis factor.

Torki and Etesami, 2020 [6] investigated the natural convection heat transport of SiO_2 /water nanofluids in a rectangular container at varied concentrations and tilt degrees. The findings demonstrated that nanofluid heat transfer characteristics did not change significantly at low concentrations. However, when the volume concentration of nanoparticles is greater than 0.005, the heat transfer coefficient declines. Roy et al. 2018[7] proposed a model for exploring the spontaneous convection of a nanofluid between two square enclosures. The flow intensity rises with the volume of nanoparticles and the Rayleigh number. The Nusselt number increases roughly linearly in the inner and outer cylinders as the nanoparticle volume concentration increases, yet the Rayleigh number increases exponentially.

A magnetic field may affect natural convection in various practical applications. Consequently, interest in the flow behavior and heat transfer mechanism of enclosures filled with electrically conducting fluids and subjected to a magnetic field has increased [8]–[16]. These investigations agree that the fluid inside the enclosure feels a Lorentz force due to the magnetic effects. This force affects both the buoyant flow field and the heat transfer rate. Mourad et al., 2021 [17] studied the natural convective flow and heat transfer in the cold wavy enclosure and the hot elliptical cylindrical. Alumina nanoparticles are added to the water to improve heat exchange. A drop in the Nusselt number values of up to 22.22 percent is offered when Ha is changed from 0 to 100.

Dogonchi et al., 2020 [13] studied the heat transfer in a square enclosure under a magnetic field and nanoparticles using natural convection. The heat transfer rate in the presence of magnetic fields on the inner wall of the annulus increases as the Rayleigh number, nanoparticle volume fraction increases, and decreases as the Hartmann number increases.

Alsabery et al., 2018 [18] studied the conjugate MHD natural convection of Al_2O_3 -water nanofluid in a square cavity with a conductive inner block. According to the findings, the heat and mass transfer mechanisms and the flow characteristics within the enclosure are substantially influenced by the

magnetic field intensity and the amount of heat generated. Employing a velocity-vorticity formulation, Reddy and Murugesan, 2017 [11] examined double-diffusive natural convection in a square cavity with an external magnetic field. The results showed that the increase from 0 to 30 of Ha had reduced Nusselt and Sherwood numbers by around 72 percent and 78 percent, respectively.

Mahmoudi, Mejri, and Omri, 2016 [16] have studied the natural convection of an Al_2O_3 -water nanofluid in two heat sinks vertically, and the horizontal walls were subjected to the magnetic field. The results showed that the heat transfer rate increases as the Hartmann number grows and the Rayleigh number increases. Furthermore, the heat transfer rate rises linearly as the solid volume percentage of nanoparticles increases. Dimitrienko and Li, 2020 [19] investigated the laminar natural convection of a non-Newtonian Carreau fluid in a square cavity with a uniform magnetic field. The work has examined the effects of the Rayleigh number (10^4 and 10^5) and the Prandtl number ($Pr=0.065$) on the cavity. The findings indicate that the heat transfer rate rises as the Hartmann number lowers and the Rayleigh number increases.

Mehran et al., 2017 [20] explored the topic of unsteady natural convection inside a square cavity separated by a flexible impermeable membrane. The cavity's horizontal walls are adiabatic, while the vertical walls are isothermal. A homogeneous magnetic field with varying orientations is applied to the cavity. The Hartmann number affects the form of the membrane and heat transport inside the hollow. The magnetic field orientation angle also has a substantial impact on the form of the membrane and heat transport inside the cavity. Liao and Li, 2021 [21] quantitatively examined natural convection inside a square cavity under an angled magnetic field, emphasizing the heat transfer transition. The findings demonstrate that increasing the magnetic field strength alters the flow field significantly. The average Nusselt number (Nu_{mean}) and the maximum streamline dropped with growing magnetic fields.

This study aims to evaluate experimentally the effects of an applied magnetic field on a nanofluid in a square cavity driven by natural convection to propose a partial answer to this difficulty. This effect will be investigated via the completion of the following tasks: synthesis and characterization of the nanofluid, fabrication of the experimental equipment, and testing of the nanofluids under a variety of experimental settings.

2. Experimental setup and procedure

The experimental apparatus was designed and implemented at Wasit University/Faculty of Engineering. A square chamber with dimensions of $100 \times 100 \times 100 \text{ mm}^3$ was built to test the reaction of a range of nanofluids to natural convection. Insulation is applied to all other walls except for two vertical walls, which are maintained at constant temperatures. It is enclosed in an insulating hardwood box to keep the cavity warm. A wire heater and a cooler device were used to achieve the steady wall temperature boundary condition. Two thermocouples were placed near the hot and cold walls to measure their temperature.

Adjustments were made to the hot wall by the wire heater, which ranged from 40°C to 55°C , and the cold wall, which ranged from 5°C to 20°C .

A magnetic field was created using permanent magnets. Removable insulating material covered the magnets, and it was designed to fit neatly into the housing above and below the cavity. Figure (1) shows the combinations of relevance in this investigation. A magnetic field line was generated in the direction of the required fluid flow, and the complete arrangement was selected to achieve this. It was decided to use

configuration (a) in order to cover the whole cavity with a magnetic field that moves with the projected fluid flow. The issue with this configuration is that the magnetic field lines go in the opposite direction to the fluid along the insulated walls. Figure 2. Schematic depiction of the experiment's setup.

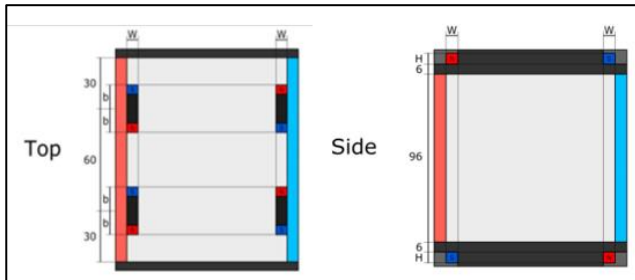


Figure 1. Configurations of permanent magnets are used for exciting the magnetic nanofluid with: (a) four magnets located on the top and bottom of the cavity.

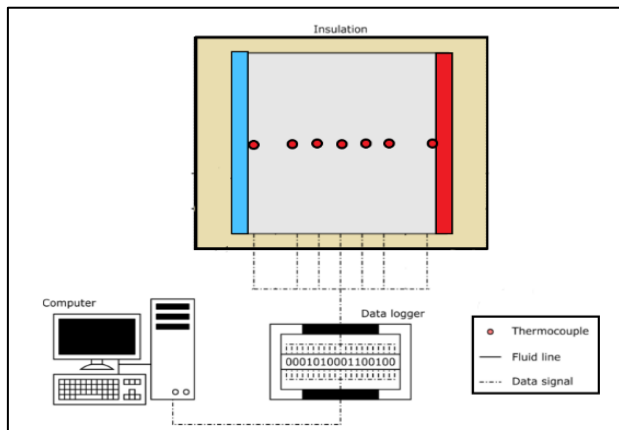


Figure 2. Schematic depiction of the experiment's setup.

2.1 Experimental procedure

The measurements were carried out in a steady-state environment. Each test case was provided adequate time to attain a steady state after the necessary adjustments in test circumstances, such as the heat flux and volume fraction of the nanofluid. Changes in flux or fluid type requiring a long time were given a deadline of 60 minutes as the maximum. For example, the temperature records for an enclosure initially kept at room temperature for $Gr = 1.21 \times 10^9$, $Ha = 0$, and $\phi = 0\%$ took the system 55 minutes to achieve a steady state when the hot plate temperature records varied by less than 1%.

2.2 Preparation of nanofluids

A two-step approach accomplishes the preparation of nanofluids. First, ultrasonic vibration (model, power sonic 410) is employed to disperse the nanopowder in the distilled water, as depicted in Figure 3, used in the current study. (Beijing Deke Daojin Science and Technology Co., Ltd.). The nanofluids are generated in the chemical measuring flask using ultrasonic vibration. The nanoparticles are precisely weighed with a computerized scale with seven numbers (OHAUS, Thornton CO). The diameter of nanoparticles of CuO is 25nm, and the density is 6500 kg/m³.

In contrast, water's density is 996.6 kg/m³. Estimated nanopowder masses are based on the percentage of particle concentration, the known density of powder, and distilled water densities (Syam Sundar and Sharma 2008) [22]. The equation for the mixture and the weights of the nanoparticles have been presented. The following formula represents this equation.

$$W_p = \frac{\phi}{(1-\phi)} \frac{\rho_p}{\rho_w} W_w \quad (1)$$

Where W denotes the mass in grams and w and p denote the water and nanoparticle, respectively. The SEM image in Figure (4) depicts the dry nanoparticles tested in this study, which have a diameter of 25 nm and a purity of 99.99 percent, according to the manufacturer's report.

All measurements were conducted in the laboratory of the Mechanical Engineering Faculty, University of Technology. The procedure and the types of equipment used in the measurements were described in detail.



Figure 3. An ultrasonic bath (Model power sonic 410) was used for nanofluid preparation.



Figure 4. SEM image of 25 nm dry OF CuO nanopowder.

Nanofluids with two volume fractions for periods ranging from 24 hours to 48 hours after synthesis are shown in Figures (5) (a)–(b).

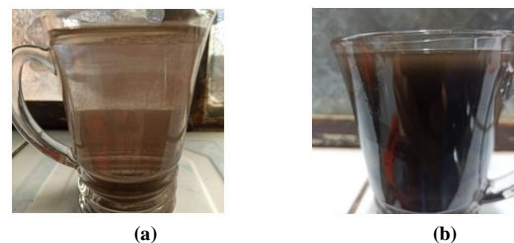


Figure 5. Stability of nanofluids, (a) CuO–DW for 1% after 48 hr, (b) CuO–DW for 1% and after 24 hr.

2.3 Data Reduction

This section briefly explains non-dimensional terminology related to natural convection-dominated instances. Also explored are certain natural convection-induced cavity flow empirical correlations. Natural convection-driven nanofluids are also included in this section.

2.4 The Natural convection in a square cavity

Consider a container with two opposing walls that are both isothermal and adiabatic at the same time. Conduction would be the most dominant heat transmission mechanism in this case if all of the buoyancy effects were removed. If buoyancy effects were considered, fluid would flow up and down, resulting in a flow of fluid from the cavity hot to the cold wall. Furthermore, while considering the shape that the heat transfer rate takes via this cavity, the following comparison to a pure conduction situation may be drawn:

$$\mathbf{q} = \mathbf{I} \times \mathbf{V} \quad (2)$$

$$\mathbf{q} = \mathbf{A} \cdot \mathbf{h} \cdot (\mathbf{T}_1 - \mathbf{T}_2) \quad (3)$$

Where A is the cross-sectional area of the flow, the temperature differences between the hot and cold walls are represented by the letters T1 and T2, respectively. When seen from a global viewpoint, heat transmission via a cavity behaves as an enhanced form of pure conduction, as demonstrated by this experiment [19].

The results of the Nusselt number are determined by:

$$Nu = \frac{hL}{k} \quad (4)$$

where H is the cavity's height and L is the distance between the hot and cold walls, Equations 1.14 and 1.15 are valid for any Pr range.

Effective thermophysical properties of the nanofluids. The dynamic viscosity was studied by Corcione (Corcione 2011) [23], who created an empirical correlation for it based on a vast quantity of experimental data from the literature. Nanoparticles with diameters ranging from 25 nm were included in the database, which was suspended in base fluids. With temperature ranges ranging from 293 K to 333 K, nanoparticle concentrations ranging from 0.001 percent to 1.5 percent were used in the experiments. It is possible to write it as follows:

$$\frac{\mu_{nf}}{\mu_f} = \frac{1}{1 - 34.87 \left(\frac{d_p}{d_f}\right)^{-0.3} \phi^{1.03}} \quad (5)$$

where μ_{nf} is the effective dynamic viscosity of the nanofluid, μ_f is the dynamic viscosity of the base fluid, and d_f is the equivalent diameter of the base fluid. The molecule is given by:

$$d_f = 0.1 \left[\frac{6M}{N\pi\rho_f} \right]^{1/3} \quad (6)$$

where M is the molecular weight, N is the Avogadro number, and ρ_f is the base fluid mass density approximated at 293 K. There is a standard variation of 1.84 percent in the preceding effective viscosity equation.

The effective thermal conductivity of hybrid nanofluids is calculated using the correlation given in the study by R.Prasher et al., 2005, [49]. There are two terms for this correlation: the first term and the dynamic part due to

Brownian motion, which is the second term. The thermal conductivity correlation used is

$$k_{eff} = (1 + AR e^m Pr^{0.333} \phi) \left[\frac{k_p + 2k_{pf} + 2(k_p - k_{pf}) \phi}{k_p + 2k_{pf} - (k_p - k_{pf}) \phi} \right] k_{pf} \quad (7)$$

The effective density of the Nanofluid is given by Pack and Cho (1998)

$$\rho_{nf} = \phi \rho_p + (1 - \phi) \rho_f \quad (8)$$

where ρ_p and ρ_f are the densities of the nanoparticles and the base fluid, respectively.

The effective specific heat at a constant pressure of the nanofluid ($c_{p,nf}$) is computed using the following equation Khanafar *et al.*, (2003)

$$C_{p,nf} = \frac{(1-\phi)(\rho c_p)_f + \phi(\rho c_p)_p}{(1-\phi)\rho_f + \phi\rho_p} \quad (9)$$

3. Result and discussion

The natural convection heat transfer properties for 1.5, 1, 0.5, and 0.1% Cu/water solutions at constant particle sizes, in a rectangular enclosure are explored experimentally in this section. The experimental work was carried out on the rectangular enclosure side walls at varying temperatures, with Ra numbers ranging from 2.76E+8 to 6.89E+8 and Hartman numbers ranging from 100 to 300.

3.1 Influence of nanoparticle concentration

The hot side of the thermal bath's enclosure had temperatures of 40 °C, 45 °C, 50 °C, and 55 °C, while the cold side had temperatures of 20 °C, 15 °C, 10 °C, and 5 °C. The fluid's temperature was measured within the cavity, along the cavity's mid-plane, under Ha=300, as shown in Figure 6. According to the volume concentration of a certain fluid, the temperature for all four thermal bath configurations (The hot-cold thermal bath temperature indicated in the legend) determined which fluid will be used. For any thermal bath arrangement, the value at $x = 0$ m corresponds to the temperature of the cold wall in the center of the wall. While the value at $x = 0.1$ m corresponds to the temperature of the hot wall in the center of the wall. Practical experiments show that the temperature of the nanofluid in the middle of the cube increases as the temperature difference between the two side walls of the enclosure increases. This is because the rotational motion of the fluid increases with increasing temperature differences. Therefore, good fluid mixing is achieved, which leads to higher fluid temperatures. It is also noted that the temperature of the nanofluid with the highest concentration beside the hot wall is the highest compared to the other nanofluid sections, while the temperature of it is the lowest beside the cold wall. This is since raising the concentration of nanomaterials improves the thermal conductivity of the fluid, and hence its heat absorption is particularly high at the hot wall.

On the contrary, the nanofluid with the highest concentration of nanoparticles has a very high loss of heat when it hits the cold wall. Moreover, the addition of CuO particles enhances the buoyancy, and the size of the vortices increases. In addition, the magnetic flux on the sidewalls of the cube attracts nanoparticles. As a result, its temperature rises when it is near a hot wall and falls when it is near a cold wall. That will be discussed in greater detail in the subsequent sections of the research.

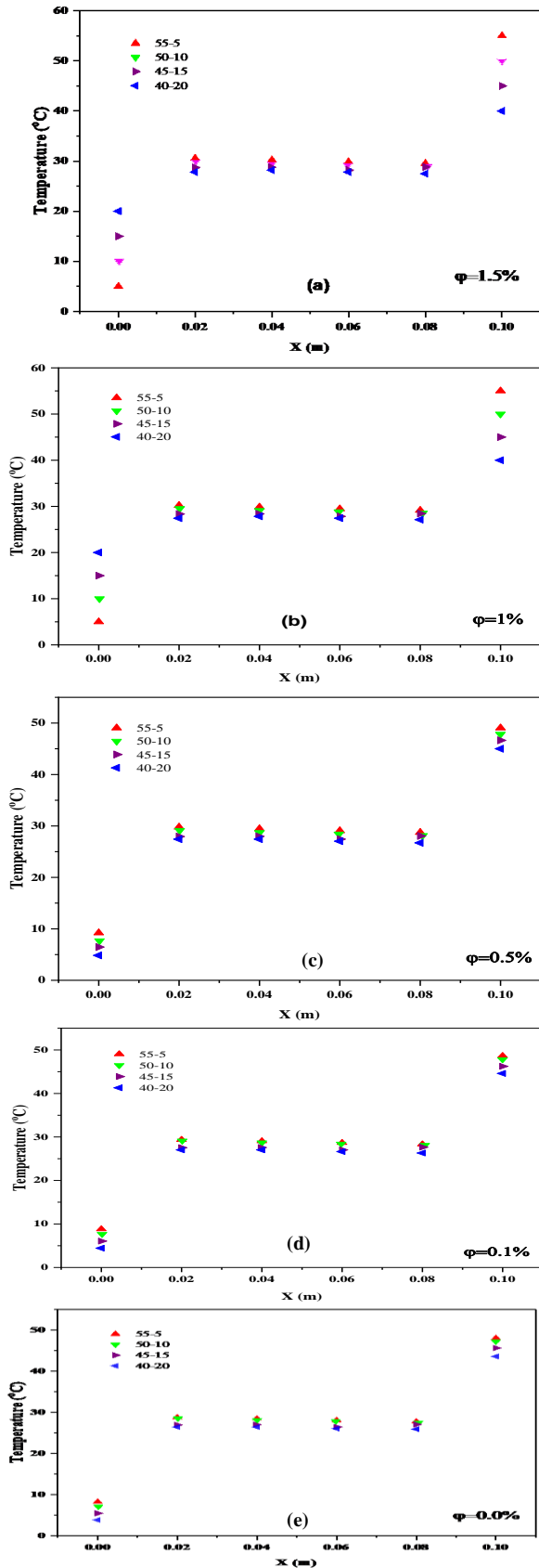


Figure 6. Fluid temperature at different CuO volume concentrations.

The information below is used to assess how much of the heat that departs from the hot side of the heat exchanger is completely transported through the system. The primary goal of managing the flow rate from the thermal baths is to minimize the disparity as much as possible. The cavity with differentially heated walls transmits all of the heat received at the hot wall to the cold wall in the steady state. Therefore, the amount of accessible heat is reduced by altering the flow rate, allowing the nanofluid to efficiently transport the bulk of the heat through the system while lowering other losses and ensuring that the system under investigation is a good approximation of the intended issue. Figure 7 depicts the heat transmission at the hot wall. In addition, the average coefficient of heat transfer for hot sides is calculated using heat transfer on the heated side. Figure 7 shows that the rate of heat transfer increases as the concentration of nanoparticles in the fluid increases when the vertical wall temperature difference is fixed for all cases. This is because the thermal conductivity of the fluid increases by increasing the concentration of nanoparticles in the fluid. In addition, Figure 7 shows that the heat transfer rate has clearly increased as the temperature difference between the hot wall and the cold wall rises because of the fluid velocity acceleration.

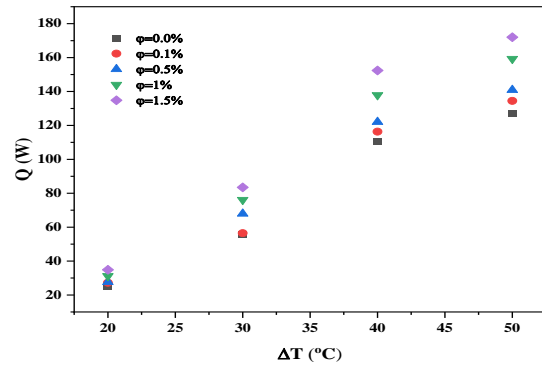


Figure 7. Heat transfer at the hot wall as a factor of the temperature difference between the hot and cold walls.

3.2 Experimental heat transfer coefficient of the nanofluid

The influence of various CuO nanoparticles distributed in the base fluid at concentrations of 0.1 %, 0.5 %, 1 %, and 1.5 % on the heat transfer coefficient at Ra values ranging from 2.76E+8 to 6.89E+8 was investigated in this section of the study. Hartman's number value has been set to 300. The experimental findings indicate that raising the Rayleigh number enhances the heat transfer coefficient when the nanofluid concentration and Hartman number remain constant. A greater Rayleigh number implies a greater flow velocity inside the rectangular container. Additionally, scattered nanoparticles in a fluid have been shown to boost its thermal conductivity. As a result, the heat transfer coefficient rises as the flow's velocity and thermal conductivity increase. The greatest improvement is 38.6% at a 1.5% concentration and Ra=6.89E+8, and the minimum improvement is 31.5% at a 1.5% concentration and Ra=2.76E+8 compared to water. As shown, the heat transfer coefficient rises slightly if the concentration of nanoparticles increases in the case of Rayleigh=2.76E+8 but increases significantly as the number of Rayleigh grows. In other words, thermal conductivity is the dominant mechanism of heat transfer at low Rayleigh numbers, which has a significant effect on the enhancement ratio. When Rayleigh is high, the natural convection heat transfer takes precedence over thermal conductivity.

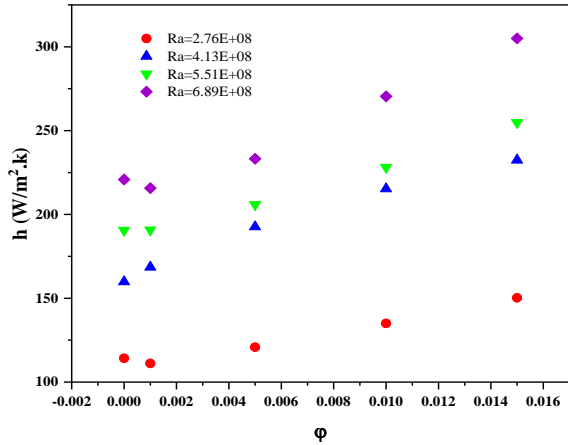


Figure 8. Effect of Ra and nanoparticles concentration of CuO on heat transfer coefficient.

3.3 Experimental Nusselt number of the nanofluid

The Nusselt number distributions of CuO nanofluid with various nanoparticle volume fractions are shown in Figure 8 at the hot wall. As predicted, the same results established for the behavior of the heat transfer coefficient apply to the behavior of the Nu. At the same Ra, the average Nu for water and nanofluids is compared. As can be seen, the Nusselt number and Rayleigh number increase as the volume proportion of nanoparticles increases. The maximum improvement is 38.6% at a 1.5% concentration and Ra=6.89E+8, and the minimum improvement is 15.7% at a 1.5% concentration and Ra=2.76E+8 compared to water.

Increased nanoparticle volume fraction increases the fluid's overall thermal conductivity and heat transfer. Increasing Rayleigh number converts heat transfer from conduction to convection, enhancing heat transfer. The presence of a high Rayleigh number disrupts the boundary layer and improves natural convection heat transfer.

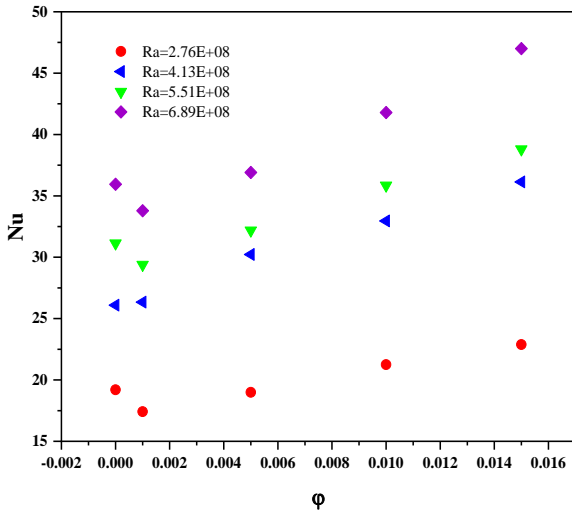


Figure 9. Effect of Ra and nanoparticle concentration of CuO on the Nusselt number.

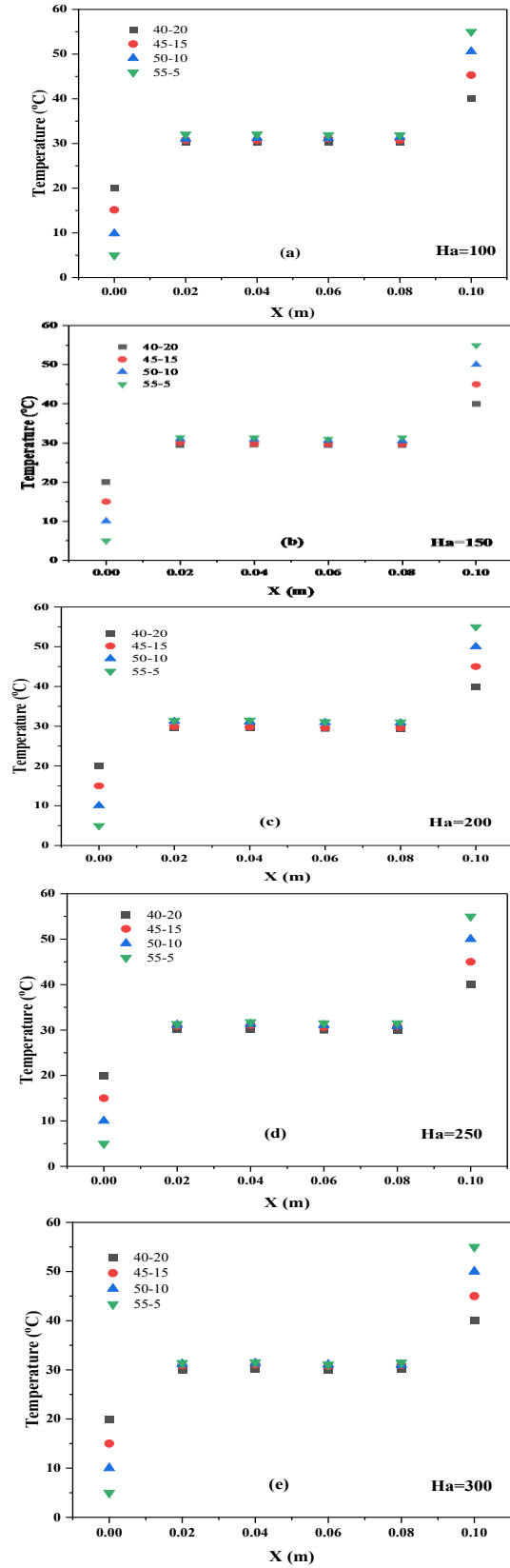


Figure 10. The influence of various magnetic fields on a nanofluid's heat transfer performance.

3.4 Experimental heat transfer coefficient of the MHD

In this section of the experiment, the impact of varying the magnetic flux values on the hot and cold walls was investigated. The magnetic flux values changed from 0 to 300. In this investigation, CuO/water nanofluid was tested at a volume concentration of 0.015, with Rayleigh's number ranging from 2.56×10^8 to 6.43×10^8 . It is clearly seen in Figure 10 that the heat transfer coefficient values increase as the Ra increases. In addition, the study shows that applying a magnetic field to the walls of a cube containing a nanofluid with two symmetrical walls, one of which is heated and the other is cold, generates two cases of heat transfer, which is either the transfer of heat by convection is dominant or vice versa, the transfer of heat by conduction is dominant. The higher the Rayleigh number, the greater the convective heat transfer; conversely, the higher the Hartman number, the stronger the heat transfer conduction and the lower the convective heat transfer. This investigation discovered that the heat transfer coefficient increases as the Rayleigh number increases, as indicated previously, and the heat transfer coefficient reduces as the Hartman number increases. In addition, it can be shown in Figure 11 that the heat transfer coefficients at $Ha=100$ and 150 are larger than the heat transfer coefficients at $Ha=0$. The maximum enhancement is 40.8% at $Ra=6.7 \times 10^8$ and $Ha=100$ compared to water at $Ha=100$ and $Ra=6.7 \times 10^8$. As previously stated, the Hartman number significantly impacts the pace at which heat transfers between two objects. The existence of Lorentz forces causes the nanoparticles in the fluid to be drawn to the wall. Since the low magnetic flux does not greatly restrict the velocity of the fluid, the absorption of heat from the nanoparticle rises as a result.

3.5 The Influence of a magnetic field

The impacts of various magnetic fields on the heat transfer performance of a nanofluid are only assessed for the 1.5 percent volume concentration scenario because this nanofluid demonstrated the greatest rise in Nu when the largest magnetic field was applied. Based on the findings in Section 4.1, there is reason to anticipate that when the other volume concentration nanofluid is utilized, the heat transfer performance will be considerably more sensitive to the magnetic field, particularly in the enhanced scenario. However, in light of the findings of (Yu et al. 2017) [24], who discovered that the stability of fluids with a lower volume concentration is poorer, the nanofluid of choice for this investigation was fluid with a 1.5 percent volume concentration, due to the likelihood of increased settling rates due to the extra magnetic pull on the nanoparticles.

The temperature degree measured on the hot side of the enclosure is 55, 50, 45, and 40 °C, while the temperature degree measured on the cold side of the enclosure is 5 °C, 10 °C, 15 °C, and 20 °C. The fluid temperature inside the cavity along the mid-plane as a function of $Ha=100, 150, 200, 250,$ and 300 is shown in Figure 10. The temperature for each of the four thermal bath configurations (described in the legend as hot-cold thermal bath temperature) utilized for a specific fluid is calculated using the volume concentration of that fluid of 0.015.

Figure 10 shows that although the fluid temperatures in the centerline of the rectangular enclosure increased as a result of the nanofluid compared with water, as mentioned earlier, the magnetic flux on the walls of the cube lowered the fluid temperatures. It also shows that temperatures decrease with increasing magnetic flux. This can be explained by the fact that the magnetic field generates Lorentz forces that inhibit the buoyancy forces caused by the heating of the liquid. Lorentz forces are perpendicular to gravitational forces in their behavior. As a result, the movement of

nanoparticles reduces the heat transfer from the hot wall to the liquid decreases, and the susceptibility of the cold wall to absorb heat from the hot liquid also decreases.

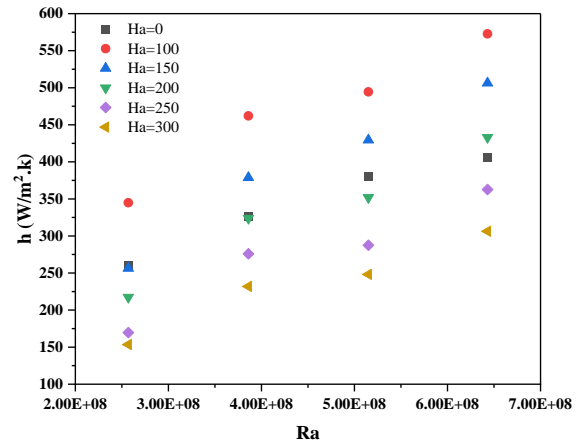


Figure 11. Effect of different Ha and Ra on Heat transfer coefficients.

3.6 Experimental nusselt number of the MHD

Figure 12 shows the change in the Nusselt number because of the Hartman and Riley values change. Fortunately, Nusselt number values gradually increase as Riley increases. The reason for this, as mentioned earlier, is the increase in the coefficient of heat transfer. It is also noted that Nusselt number values decrease as Hartman numbers increase by more than 150. The maximum enhancement is 28.5% at $Ra=6.7 \times 10^8$ and $Ha=100$ compared to water at $Ha=100$ and $Ra=6.7 \times 10^8$. This is due to the fact that heat transfer in these cases is caused by the control of heat transfer by conduction and the decrease of heat transfer by convection, in contrast to the case of Hartman numbers values. Increasing the intensity of the magnetic flux limits the speed of flow and buoyancy.

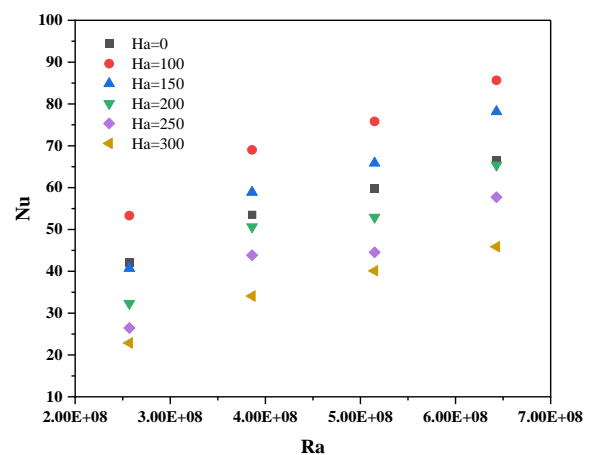


Figure 12. Effect of different Ha and Ra values on Nusselt number

4. Conclusion

Numerical findings can be summarized as follows:

1. The addition of CuO particles enhances the buoyancy, and the sizes of the vortices increase.
2. The magnetic flux on the sidewalls of the cube attracts nanoparticles, thereby increasing its temperature at the hot wall and decreasing it at the Cold Wall.
3. The rate of heat transfer increases as the concentration of nanoparticles in the fluid increases when the vertical wall temperature difference is fixed.
4. The heat transfer coefficient rises slightly when the concentration of nanoparticles increases in the case of Rayleigh=2.76E+8 but increases significantly as the number of Rayleigh grows.
5. The Nusselt number grows as the volume percentage of nanoparticles and the Rayleigh number increase.
6. The magnetic flux on the walls of the cube lowered the fluid temperatures.
7. The heat transfer coefficient increased with the rise of the Rayleigh number, and on the contrary, the values of the heat transfer coefficient decreased with the increase in the importance of the Hartmann number.
8. The heat transfer coefficients at Ha=100 and 150 are larger than the heat transfer coefficients at Ha= 0.
9. Nusselt number values decrease as Hartmann numbers increase more than 150.

REFERENCES

- [1] X.-Q. Wang and A. S. Mujumdar, "Heat transfer characteristics of nanofluids: a review," *Int. J. Therm. Sci.*, vol. 46, no. 1, pp. 1–19, 2007.
- [2] U. S. Choi, "Enhancing thermal conductivity of fluids with nanoparticles, Development and Applications of Non-Newtonian flows edited by Siginer, DA and Wang, HP, EFD-Vol. 231/MD-Vol. 66," 1995.
- [3] A. H. Pordanjani, S. M. Vahedi, F. Rikhtegar, and S. Wongwises, "Optimization and sensitivity analysis of magnetohydrodynamic natural convection nanofluid flow inside a square enclosure using response surface methodology," *J. Therm. Anal. Calorim.*, vol. 135, no. 2, pp. 1031–1045, 2019.
- [4] R. Mohebbi, M. Izadi, H. Sajjadi, A. A. Delouei, and M. A. Sheremet, "Examining of nanofluid natural convection heat transfer in a Γ -shaped enclosure including a rectangular hot obstacle using the lattice Boltzmann method," *Phys. A Stat. Mech. its Appl.*, vol. 526, p. 120831, 2019, doi: <https://doi.org/10.1016/j.physa.2019.04.067>.
- [5] M. Izadi, G. Hoghoughi, R. Mohebbi, and M. Sheremet, "Nanoparticle migration and natural convection heat transfer of Cu-water nanofluid inside a porous undulant-wall enclosure using LTNE and two-phase model," *J. Mol. Liq.*, vol. 261, pp. 357–372, 2018, doi: <https://doi.org/10.1016/j.molliq.2018.04.063>.
- [6] M. Toriki and N. Etesami, "Experimental investigation of natural convection heat transfer of SiO₂/water nanofluid inside the inclined enclosure," *J. Therm. Anal. Calorim.*, vol. 139, no. 2, pp. 1565–1574, 2020.
- [7] N. C. Roy, "Natural convection of nanofluids in a square enclosure with different shapes of inner geometry," *Phys. Fluids*, vol. 30, no. 11, p. 113605, 2018.
- [8] R. J. Moreau, *Magnetohydrodynamics*, vol. 3. Springer Science & Business Media, 1990.
- [9] A. Bennia and M. N. Bouaziz, "CFD modeling of turbulent forced convective heat transfer and friction factor in a tube for Fe₃O₄ magnetic nanofluid in the presence of a magnetic field," *J. Taiwan Inst. Chem. Eng.*, vol. 78, pp. 127–136, 2017.
- [10] T. S. Devi, C. V. Lakshmi, K. Venkatadri, and M. S. Reddy, "Influence of external magnetic wire on natural convection of non-Newtonian fluid in a square cavity," *Partial Differ. Equations Appl. Math.*, vol. 4, p. 100041, 2021.
- [11] N. Reddy and K. Murugesan, "Magnetic field influence on double-diffusive natural convection in a square cavity—A numerical study," *Numer. heat Transf. part A Appl.*, vol. 71, no. 4, pp. 448–475, 2017.
- [12] S. M. Aminossadati, A. Raisi, and B. Ghasemi, "Effects of magnetic field on nanofluid forced convection in a partially heated microchannel," *Int. J. Non. Linear. Mech.*, vol. 46, no. 10, pp. 1373–1382, 2011, doi: [10.1016/j.ijnonlinmec.2011.07.013](https://doi.org/10.1016/j.ijnonlinmec.2011.07.013).
- [13] A. S. Dogonchi, T. Tayebi, A. J. Chamkha, and D. D. Ganji, "Natural convection analysis in a square enclosure with a wavy circular heater under magnetic field and nanoparticles," *J. Therm. Anal. Calorim.*, vol. 139, no. 1, pp. 661–671, 2020.
- [14] M. M. Rashidi, M. Nasiri, M. Khezerloo, and N. Laraqi, "Numerical investigation of magnetic field effect on mixed convection heat transfer of nanofluid in a channel with sinusoidal walls," *J. Magn. Magn. Mater.*, vol. 401, pp. 159–168, 2016, doi: [10.1016/j.jmmm.2015.10.034](https://doi.org/10.1016/j.jmmm.2015.10.034).
- [15] P. Y. Lee, K. Ishizaka, H. Suematsu, W. Jiang, and K. Yatsui, "Magnetic and gas sensing property of nanosized NiFe₂O₄ 4 powders synthesized by pulsed wire discharge," *J. Nanoparticle Res.*, vol. 8, no. 1, pp. 29–35, 2006, doi: [10.1007/s11051-005-5427-z](https://doi.org/10.1007/s11051-005-5427-z).
- [16] A. Mahmoudi, I. Mejri, and A. Omri, "Study of natural convection in a square cavity filled with nanofluid and subjected to a magnetic field," *Int. J. Heat Technol.*, vol. 34, no. 1, pp. 73–79, 2016.
- [17] A. Mourad, A. Aissa, F. Mebarek-Oudina, W. Al-Kouz, and M. Sahnoun, "Natural convection of nanofluid from elliptic cylinder in wavy enclosure under the effect of uniform magnetic field: numerical investigation," *Eur. Phys. J. Plus*, vol. 136, no. 4, pp. 1–18, 2021.
- [18] A. I. Alsabery, T. Tayebi, A. J. Chamkha, and I. Hashim, "Effects of two-phase nanofluid model on natural convection in a square cavity in the presence of an adiabatic inner block and magnetic field," *Int. J. Numer. Methods Heat Fluid Flow*, 2018.
- [19] Y. I. Dimitrienko and S. Li, "Numerical simulation of MHD natural convection heat transfer in a square cavity filled with Carreau fluids under magnetic fields in different directions," *Comput. Appl. Math.*, vol. 39, no. 4, pp. 1–26, 2020.
- [20] S. A. M. Mehryan, M. Ghalambaz, M. A. Ismael, and A. J. Chamkha, "Analysis of fluid-solid interaction in MHD natural convection in a square cavity equally partitioned by a vertical flexible membrane," *J. Magn. Magn. Mater.*, vol. 424, pp. 161–173, 2017.
- [21] C.-C. Liao and W.-K. Li, "Assessment of the magnetic field influence on heat transfer transition of natural convection within a square cavity," *Case Stud. Therm. Eng.*, vol. 28, p. 101638, 2021.
- [22] M. Corcione, "Empirical correlating equations for predicting the effective thermal conductivity and dynamic viscosity of nanofluids," *Energy Convers. Manag.*, vol. 52, no. 1, pp. 789–793, 2011.